Physics and Imaging in Radiation Oncology 33 (2025) 100697

Contents lists available at ScienceDirect

Physics and Imaging in Radiation Oncology

journal homepage: www.sciencedirect.com/journal/physics-and-imaging-in-radiation-oncology

Technical Note

Nontoxic generalized patient shielding devices for total skin electron therapy

Clinton Gibson *, Joseph B. Schulz, Amy Yu, Piotr Dubrowski, Lawrie Skinner

Department of Radiation Oncology, Stanford University, 875 Blake Wilbur Drive, Stanford, CA

ARTICLE INFO

Keywords:
Total skin electron irradiation
3D printed bolus
Mycosis fungoides

ABSTRACT

This study evaluates alternative shielding materials to lead for protecting the scalp and nails during total skin electron irradiation. We tested a silicone helmet, tungsten-doped silicone mittens, and planar aluminum and copper shields. The helmet and mittens were created using 3D modeling software and fused filament fabrication printing, while the planar shields were machined and assembled with printed hardware. Transmission measurements showed transmission rates of 4.5%–6.8% for the mittens, 5.8%–9.1% for the helmet, and 7.5% for the planar shields. The silicone-based devices improve comfort and usability, and slight design changes can enhance coverage and application.

1. Introduction

While total skin electron irradiation (TSEI) is successfully used to treat Mycosis fungoides (MF) T-cell cutaneous lymphoma [1–5], common toxicities include partial or complete alopecia and nail loss in the range of 10 to 36 Gy to the skin [6–8]. To minimize toxicity, hands, feet, whole head or just the scalp may be shielded for hair preservation, nail preservation, cataract avoidance and other needs. Lead gloves, lead helmets, or face and foot shields are often used to provide shielding. The lead, however, adds significant risks to patients and staff, who are handling several kilograms of lead objects daily. There is no safe exposure level of lead and even micrograms in the blood are known to be deleterious to health [9].

Existing Lead-free shielding solutions for the scalp include molded thermoplastic and commercial bolus [10]. Patient specific and generic non-toxic shielding solutions include a milled wax polyethylene helmet [11]. Generic head shields using a 3D printed mold and silicone have also been reported [12,13]. Our previous work involved preparing a patient specific, 3D printed helmet made from polylactic acid (PLA) plastic fitted with 3 mm thick commercial bolus, while patient specific silicone boluses made from filling 3D printed molds were demonstrated by Canters et al. and Chiu et al. [13–15]. Silicone offers mechanical flexibility and density close to tissue, low backscatter, and low Bremsstrahlung. Our study aims to build upon this prior work by introducing generalized silicone helmets, silicone mittens doped with tungsten powder, and non-toxic aluminum and copper foot and head shields for clinical TSEI treatments. While this work focusses on solutions for the Stanford TSEI six dual beam technique [1], the shielding geometry and requirements are broadly transferable to rotational TSEI and other techniques [2,3].

2. Materials and methods

2.1. On-patient shield designs and manufacture

The lead-free gloves (Fig. 1A and 1B) were made by combining a 3D hand model from free3d.com database and the contour of a real hand using Fusion 360 and Meshmixer software (Autodesk, San Francisco, CA). Meshmixer was then used to create a mold for a glove with 10 mm thick walls. The mold was 3D printed using PLA filament and an Ultimaker S5 3D printer (Ultimaker, Utrecht, Netherlands). Tungsten powder (Atlantic Equipment Engineers, Upper Saddle River, NJ) was mixed with silicone rubber (SORTA-Clear™ 37, Smooth-On, Macungie, PA) for volume-efficient shielding in a ratio of 2:1 by weight with a target density of 2.5 g/cc. The silicone and tungsten mixture were poured in stages such that settling of the tungsten powder was limited to each poured segment.

The helmet was created by expanding the contour of a previous patient's head by 22 mm and refining it into a helmet shape with Meshmixer. A conical hole was placed in the top of the helmet with Meshmixer where a 3D printed hook was installed to hang the helmet by a rope and improve wearability. 23 mm of equivalent water thickness is

* Corresponding author.
E-mail address: cgibson@stanfordhealthcare.org (C. Gibson).

https://doi.org/10.1016/j.phro.2025.100697
Received 12 August 2024; Received in revised form 28 December 2024; Accepted 9 January 2025
Available online 18 January 2025

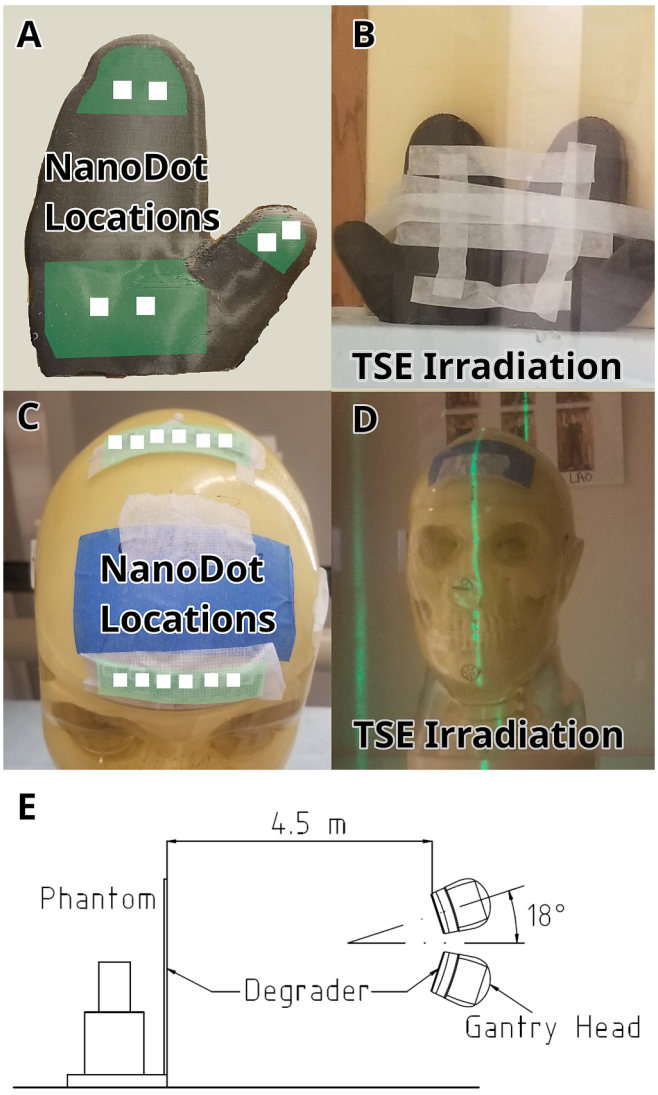

Fig. 1. OSLD placement on the head phantom and gloves (A and C) and their placement in the TSEI booth (B and D). The experimental setup is illustrated in E.

required to attenuate 90 % of the incident beam, and the helmet was designed to include a 1 mm margin for 24 mm of equivalent water thickness when filled with silicone rubber that has a density of 1.1 g/cc (see section 2.3 for detail) [13]. To save weight, the top of the helmet was thinned to 16 mm, since the full thickness was not required due to the obliquity of the fields. The silicone rubber was poured all at once because of the lack of tungsten powder (see section 2.3).

2.2. Planar shield design and manufacture

The foot and head shields are composed of 9.35 mm thick aluminum 6061 alloy (McMaster-Carr) and 1.57 mm thick copper 110 alloy sheets (McMaster-Carr) sandwiched together by 3D printed fasteners. Aluminum was chosen due to its low cost and low atomic number (Z) of 13, which minimizes bremsstrahlung creation, as well as its strength and machineability. Copper was added to the upstream side to provide slightly improved attenuation of photons due to its greater atomic number, while the Aluminum can absorb electrons and any copper k-edge fluorescence generated. Using the general energy loss rule of 2 MeV/cm of water, the 0.9 cm of aluminium and the 0.15 cm of copper were expected to roughly stop electron beams up to 6 MeV, as shown in Equation 1 in the supplementary equations.

2.3. Transmission measurements of on-patient shields and glove homogeneity

Transmission measurements were performed in a TSEI booth 4.5 m from the radiation source (Fig. 1E). The gloves were irradiated with a Varian TrueBeam and 4000 MU of a 9 MeV high dose rate electron beam, that has been degraded to 4.6 MeV through two PMMA degraders (total thickness 1.6 mm) and 4.5 m of air. Two gantry angles of 72 and 108 degrees were used. This setup optimizes skin dose while reducing penetration [13]. Two OSL dosimeter nanoDots (Landauer, Glenwood, IL) were taped to 1 cm thick wax and placed in the fingertips, thumb, and palm of the gloves and compared to six nanodots taped to the surface of 10 cm of solid water placed vertically in the booth (Fig. 1A and 1B). Each nanodot was readout three times. The transmission through the helmet was measured by placing six nanodots along the forehead and on top of an anthropogenic head phantom (CyberKnife® Head and Neck Phantom, Accuray Madison, WI, USA), see Fig. 1C and 1D. The orientation of the head phantom was chosen to mimic the AP positions of the Stanford "6 dual field" technique for a total of 12,000 MU [1]. Homogeneity of the gloves were checked by placing each glove on the EPID imager at 110 SID and taking a 6 MV portal image. The pixel intensities through the gloves in five regions of interest in the thumb, palm, and fingers were measured with ImageJ (ImageJ U.S., National Institutes of Health, Bethesda, Maryland). The interquartile range, median, and robust measure of scale (S_n) were then calculated for each region. S_n describes the spread around the median of skewed data like the standard deviation does for a normally distributed population [16]. See supplemental Figs. 2 and 3 for visual representations of the data.

2.4. Transmission measurements of planar shields

Transmission measurements for the non-toxic head and foot shields were made using an Exradin A10 ion chamber (Standard Imaging, Middleton, WI, USA) with 500 MU of high dose rate 9 MeV electrons delivered at 108 and 72 degrees. The transmission for each non-toxic shield was compared to the prior lead shield which consisted of 3 mm thick lead placed between two sheets of 5 mm thick plywood. Surface dose and 5 mm deep measurements were made to assess both the dose delivered to skin and tissue at 5 mm depth. Measurements were made with the surface of the solid water phantom 20 cm behind the spoiler, as shown in supplemental Fig. 1.

2.5. Bremsstrahlung measurements of planar shields

The degraded electron beam was found to have an energy of 4.6 MeV at the phantom surface from depth dose measurements [13]. A total of 5 cm of solid water was placed in front of the ion chamber to determine the amount of Bremsstrahlung radiation transmitted at a depth beyond the range of the electrons. This transmission is expressed as the ratio of charge produced between an open and shielded beam and can be found in Table 1.

Table 1
Transmission measurements for nontoxic and lead head and foot shields, all uncertainties are less than 0.3%. Transmission is an average of gantry angles 72 and 108.

Measurement Depth [cm]	Wood and Lead Shield Transmission [%]	Copper and Aluminum Shield Transmission [%]
Surface	8.5 %	7.5 %
0.5 cm	5.4 %	4.8 %
5.0 cm	6.1 %	6.1 %

3. Results

3.1. Transmission measurements of on-patient shields, density and glove homogeneity

The final density of the gloves was found to be 2.40 g/cc with an equivalent water thickness of 24 mm. The dose delivered to the six nanodots in each glove was averaged and compared to the average dose delivered to the unshielded nanodots for transmission measurements (see Fig. 1 for nanodot locations). The left-hand glove transmitted 4.5 % while the right-hand glove transmitted dose was 6.8 %. The 24 mm water equivalent thick silicone helmet transmitted 9.1 % at the forehead and 5.8 % of the delivered dose along the top. The variable homogeneity of the gloves can be illustrated by the median pixel values of the thumb, fingers, and palms of each glove. For example, the median between the palm and fingers of the right hand glove differ by 21.5 % and 17.5 % in the left and right hand gloves (see supplemental Table 1 for more detail).

3.2. Transmission and Bremsstrahlung measurements of planar shields

The transmission measurements of the non-toxic planar head and foot shields are summarized in Table 1. The copper and aluminum provided comparable shielding to the wood and lead shields, with 7.5 % of the dose delivered to the surface and 4.8 % of the dose found at 5 mm below the surface. The transmission of Bremsstrahlung radiation was identical to the conventional shields.

4. Discussion

The introduction of tungsten doped silicone gloves represents a new avenue for shielding hands and nails during TSEI without the use of lead. This work has demonstrated the ability to reduce the dose delivered to fingertips to less than 1 Gy during a 12 Gy treatment using the Stanford technique, reducing the chances of dystrophy and nail loss [6]. One limitation of compound tungsten silicone mixtures is homogeneity, as the tungsten powder tends to settle under gravity as the liquid silicone rubberizes, this was minimized in the manufacture (see methods 2.1). Despite the variation in intensity in the portal images (see section 3.1), these only reflect a change in transmission of 3.2 %, and each glove shielded over 90 % of the incident beam. The small 1–3 % discrepancy between left and right hand gloves is assumed to be a combination of nanodot uncertainty. The manufacturer stated absolute dose uncertainty of these nanodots is 5 %. Further our clinical commissioning data, from hundreds of repeated readings in known dose conditions, confirms the nanodot uncertainties are a combination of calibration error (3–5 %), readout noise (1–2 %), energy dependency (1–2 %). Imprecise measurement position (approx. 2 mm uncertainty), and the glove homogeneity add further uncertainties. The current design has the back side of the hand exposed. Further full coverage designs may be pursued using the same method.

The silicone helmet presented here offers an advantage over previous hard plastic 3D printed helmets by negating the need for additional Superflab for patient comfort [10]. The addition of a 3D printed hook to the design also allows the 2 kg helmet weight to be supported with rope, reducing the burden on the patient. Elmahmoud et al. demonstrated the use of a similar patient-specific polyethylene helmet that weighed 1.3 kg [11]. However, our facility's use of a higher energy beam produced 4.6 MeV electrons that required a thicker helmet to achieve similar shielding results. The primary drawback of our approach is that not all facilities may have access to a 3D printer, but the low cost of commercially available printers makes these methods a viable option for clinics that wish to manufacture patient specific devices.

Sterilization and or disinfection of the on-patient devices is a concern for clinical use. The silicone may be steam-sterilized in an autoclave, or it can also be able to be wiped with isopropyl alcohol for disinfection. The planar head and foot shields are not in direct contact with the patient, making sterilization less critical, but may be wiped down with isopropyl alcohol for disinfection.

The non-toxic planar head and foot shields presented here demonstrate the feasibility of a simple and affordable alternative to lead shields. Shin et al. created a thimble shaped head shield made from silicone for a 6 MeV electron beam, but the authors noted how the 4.7 kg device may make it too heavy to be placed on a patient's head [12]. Our head shield acts as a direct replacement to lead shields that can be hung in the path of the beam without needing to be worn. The measurements made at 5 cm depth demonstrated that there was no difference in Bremsstrahlung contamination between the two shielding types. This can be explained as most Bremsstrahlung comes from the linac head, with the shields providing a much smaller Bremsstrahlung contribution. Future work in non-toxic patient shielding could include generating patient specific shields, as well as tungsten filled silicone internal shields for the oral cavity.

CRediT authorship contribution statement

Clinton Gibson: Investigation, Data curation, Formal analysis, Writing – original draft. **Joseph B. Schulz:** Visualization, Investigation, Writing – review & editing. **Amy Yu:** Project administration, Supervision, Writing – review & editing. **Piotr Dubrowski:** Supervision, Writing – review & editing. **Lawrie Skinner:** Conceptualization, Project administration, Supervision, Writing – review & editing.

Declaration of competing interest

The authors declare the following financial interests/personal relationships which may be considered as potential competing interests: The work associated with our submission was funded by internal Stanford Healthcare quality improvement (SQIMM) awards.

Appendix A. Supplementary data

Supplementary data to this article can be found online at https://doi.org/10.1016/j.phro.2025.100697.

References

[1] Hoppe R, Fuks Z, Bagshaw M. Radiation therapy in the management of cutaneous T-cell lymphomas. Cancer Treat Rep 1979;63(4):625–32. PMID: 87276.
[2] Tetenes P, Radiology GP. Comparative study of superficial whole body radiotherapeutic techniques using a 4-MeV nonangulated electron beam. Radiology 1977;122(1):219–26. https://doi.org/10.1148/122.1.219.
[3] Delinikolas P, Patatoukas G, Kouloulias V, Dilvoi M, Plousi A, Efstathopoulos E, et al. A novel Hemi-Body Irradiation technique using electron beams (HBe-). Phys Med 2018;46:16–24. https://doi.org/10.1016/j.ejmp.2017.12.022.
[4] Specht L, Debaja B, Illidge T, Wilson L, Hoppe R. Modern radiation therapy for primary cutaneous lymphomas: field and dose guide. Int J Radiat Oncol Biol Phys 2015;92(1):32–9. https://doi.org/10.1016/j.ijrobp.2015.01.008.
[5] Chowdhary M, Chhabra A, Kharod S, Marwaha G. Total skin electron beam therapy in the treatment of mycosis fungoides: a review of conventional and low-dose regimens. Clin Lymphoma Myeloma and Leuk 2016;16(12):662–71. https://doi.org/10.1016/j.clml.2016.08.019.
[6] Desai K, Pezner R, Lipsett J, Vora N, Luk K, Wong J, et al. Total skin electron irradiation for mycosis fungoides: relationship between acute toxicities and measured dose at different anatomical sites. J Radiat Oncol Biol Phys 1988;15:641–5. https://doi.org/10.1016/0360-3016(88)90306-9.
[7] Grandi V, Simontacchi G, Grassi T, Pileri A, Pimpinelli N. Short term efficacy and safety of total skin electron beam therapy in mycosis fungoides: review and meta-analysis. Dermatol Therapy 2022;35(11):e15840. https://doi.org/10.1111/dth.15840.
[8] Breneman D, Breneman A, Ballman E, Breneman J. Long-term effects of total skin electron beam therapy for mycosis fungoides on hair and nail loss and regrowth. J Dermatol Treat 2022;33(4):1975–8. https://doi.org/10.1080/09546634.2021.1906398.
[9] Vorvolkaos T, Arseniou S, Samakouri M. There is no safe threshold for lead exposure: A literature review. Psychiatriki 2016;27:204–14. https://doi.org/10.22365/jpsych.2016.273.204.
[10] Patel C, Ding G, Kirschner A. Scalp-sparing total skin electron therapy in mycosis fungoides: case report featuring a technique without lead. Pract Radiat Oncol 2017;7:400–2. https://doi.org/10.1016/j.prro.2017.03.009.

[11] Elmahmoud Z, Gunther J, Christopherson K. A Simple solution to create a custom scalp-sparing helmet to prevent alopecia in patients undergoing total skin electron beam therapy for cutaneous T cell lymphoma. Clin Transl Radiat Oncol 2023;38:53–6. https://doi.org/10.1016/j.ctro.2022.10.005.

[12] Shin WG, Lee SY, Jin H, Kang S, Kim J, Jung S. Development and evaluation of a thimble-like head bolus shield for hemi-body electron beam irradiation technique. J. Radiat. Prot. Res. 2022;47(3):152–7. https://doi.org/10.14407/jrpr.2022.00010.

[13] Rahimy E, Skinner L, Kim Y, Hoppe R. Technical report: 3D-printed patient-specific scalp shield for hair preservation in total skin electron beam therapy. Tech Innov and Patient Support in Radiat Oncol 2021;18:12–5. https://doi.org/10.1016/j.tipsro.2021.03.002.

[14] Chiu T, Tan J, Brenner M, Gu X, Yang M, et al. Three-dimensional printer-aided casting of soft, custom silicone boluses (SCSBs) for head and neck radiation therapy. Pract Radiat Oncol 2018;8:167–74. https://doi.org/10.1016/j.prro.2017.11.001.

[15] Canters R, Lips I, Wendling M, Kusters M, Zeeland M, et al. Clinical implementation of 3D printing in the construction of patient specific bolus for electron beam radiotherapy for non-melanoma skin. Radiother Oncol 2016;121:184. https://doi.org/10.1016/j.radonc.2016.07.011.

[16] Rousseeuw P, Croux C. Alternatives to the median absolute deviation. J Am Stat Assoc 1993;88(424):1273–83. https://doi.org/10.1080/01621459.1993.10476408.